Polymer Journal, Vol. 37, No. 1, pp. 21–29 (2005)

Analysis of ^{13}C NMR Chemical Shielding and XPS for Cellulose and Chitosan by DFT Calculations Using the Model Molecules

Sebastian DANIELACHE,[1] Motohiro MIZUNO,[1] Shingo SHIMADA,[1] Kazunaka ENDO,[1,†] Tomonori IDA,[1] Kazuchiyo TAKAOKA,[2] and Ernst Z. KURMAEV[3]

[1]*Department of Chemistry, Faculty of Science, Kanazawa University, Kakuma-machi, Kanazawa 920-1192, Japan*
[2]*Tsukuba Research Center, Mitsubishi Paper Mills, Ltd., Wadai, Tsukuba 300-42, Japan*
[3]*Institute of Metal Physics, Russian Academy of Sciences-Ural Division, 620219 Yekaterinburg GSP-170, Russia*

(Received August 26, 2004; Accepted October 1, 2004; Published January 15, 2005)

ABSTRACT: ^{13}C NMR chemical shielding and XPS of cellulose and chitosan were analyzed by deMon DFT calculations using the model dimers. The calculated ^{13}C chemical shifts of (α-D-glucose, β-D-glucose, and β-D-glucosamine) and cellobiose with DZVP basis are in considerably good accordance with the experimental values in the average absolute deviations (AAD) of $\pm$3.1 and 2.0 ppm, respectively. The calculated shifts of the dimer models for cellulose and chitosan also correspond well to the experimental ones of both solid biopolymers in the AAD of $\pm$3.1 ppm. In order to simulate the valence XPS and to calculate core-electron binding energies (CEBE)s of cellulose and chitosan, we used the restricted diffuse ionization (rDI) and generalized transition-state (GTS) methods, respectively, due to Slater's transition-state (TS) concept. The simulated valence spectra of the dimer models showed good agreement with the experimental ones of cellulose and chitosan. We also estimated as 5.9 and 5.7 eV for ***WD*** (work function and the other energies) values of cellulose and chitosan, respectively from the differences between calculated CEBE values for the model molecules and experimental ones on the solid polymers. [DOI 10.1295/polymj.37.21]

KEY WORDS ^{13}C NMR Chemical Shielding / X-ray Photoelectron Spectra / DFT Calculations / Saccharide / Amino-Sugar /

It is well-known that cellulose is one of the most abundant natural polymers which has the biological functions of providing cells with mechanical strength and framework. One found cellulose many important applications in areas such as food, drug-delivery systems, and in textile and pulping-paper industries. The elucidation of the structural and dynamic properties of cellulose is, therefore, fundamental to understanding its role in plant cell walls and its functionality in applications. On the other hand, chitosan is especially known as a most powerful adsorbent of natural origin and widely used for the prevention of water pollution by highly toxic chlorinated aromatic compounds and metal ions.[1] It is easily prepared from chitin by deacetylating its acetoamide groups with a strong alkaline solution. Chitosan is inexpensive, environmentally benign, harmless to humans, and a hugely obtainable biomass, and makes it very promising and attracting for use in many applications. As so far as we know, no one currently still demonstrates the fundamental studies on the electronic state of the two biopolymers (cellulose and chitosan) from both experimental and theoretical viewpoints.

Studies of NMR and XPS properties in organic compounds contain a lot of valuable information concerning the nature of chemical bonds. The former studies of magnetic properties provide information about the roles of angular momentum of electrons in the chemical bonds. The latter XPS gives precise information on the electronic states involving the individual functional group of organic compounds. In our previous studies on ^{13}C NMR and XPS of organic compounds,[2–6] we performed the better assignments for ^{13}C NMR signals and the core and valence electron spectra by ab initio MO and DFT calculations, respectively.

In the present work, we select cellulose and chitosan for study of ^{13}C NMR and X-ray photoelectron spectra (XPS) from the two following reasons, and perform the analysis of spectra for the biopolymers by deMon DFT[7] calculations using the model dimers. It is well known an important role of the electronic structure in the formation of properties of biological molecules. To understand the changes in adsorption behavior of chemically modified biopolymers, cellulose and chitosan (crosslinked biopolymers), it is necessary at first to study the chemical bonding of unmodified cellulose and chitosan. On the other hand, cellulose and chitosan have a compact geometrical structure convenient for DFT calculations and possessing different oxygen and carbon atoms based functional groups that make it suitable model object for study of NMR and XPS.

[†]To whom correspondence should be addressed (endo@wriron1.s.kanazawa-u.ac.jp).

EXPERIMENTAL

We used commercially available cellulose (Sigma Chemical Co., Inc), and chitosan (Wako Chemical Co., Inc), respectively. They were pressed into the pellets before XPS measurements.

The XPS of the pellets for cellulose and chitosan were obtained on a PHI 5400MC ESCA spectrometer, using monochromatized Al Kα radiation. The spectrometer was operated at 600 W, 15 kV, and 40 mA, and the photon energy was 1486.6 eV. A pass energy of 71.55 eV was used for high resolution scans in a valence band analysis (50 eV of range). The angle between the X-ray source and analyzer was fixed at 45°. Spot size was 3 × 1 mm. Dispersion compensation yielded an instrumental resolution of 0.5 eV from full width at half-maximum for the Ag 3d line of silver. Multiscan averaging on a multichannel analyzer was used for the valence band region, although a very low photoelectron emission cross-section was observed in this range. Gold of 2.0 nm thick was deposited on the pellets of the samples using ion sputter unit (Hitachi E 1030) for scanning electron microscope. A low energy electron flood gun was used in order to avoid any charging effect on the surface of the sample. We used the Au 4f core level of the gold decoration on the samples as a calibration reference. The C 1s line positions of $-CH_2OH$ groups in the samples could be fixed at 286.7 eV for cellulose and chitosan, respectively.

For the ^{13}C NMR spectra, we referred to experimental results of (α-D-glucose, β-D-glucose, and β-D-glucosamine),[8–10] cellobiose,[11] cellulose,[11] and chitosan.[12]

THEORETICAL BACKGROUND

NMR Chemical Shielding Tensor

We used the shielding tensor equation by the sum-over-states DFT perturbation theory. The shielding tensors[13] σ_{uv} (the notations $u, v = \{x, y, z\}$) are expressed as

$$\sigma_{uv} = \sigma_{uv}^{\mathrm{d}} + \sigma_{uv}^{\mathrm{p0}} + \sigma_{uv}^{\mathrm{p1}}, \tag{1}$$

$$\sigma_{uv}^{\mathrm{d}} = 2\sum_{k}\langle k|h_{uv}^{11}|k\rangle, \tag{2}$$

$$\sigma_{uv}^{\mathrm{p0}} = -2\sum_{k}\sum_{j}\langle k|h_{u}^{01}|j\rangle\langle j|(\Lambda_j - \Lambda_k)_v|k\rangle, \tag{3}$$

$$\sigma_{uv}^{\mathrm{p1}} = -4\sum_{k}\sum_{a}\langle k|h_{u}^{01}|a\rangle\beta_{ak}(v), \tag{4}$$

with

$$h_u^{01} = -\frac{1}{c}\frac{\ell_{Nu}}{|\boldsymbol{r} - \boldsymbol{R}_N|^3}, \tag{5}$$

where $\boldsymbol{R}_N$ is the position of the nucleus N. The notation ℓ_{Nu} is

$$\ell_{Nu} = \{(\boldsymbol{r} - \boldsymbol{R}_N) \times \nabla\}_u. \tag{6}$$

The hamiltonian h_u^{11} gives

$$h_u^{11} = \frac{1}{2c^2}\frac{(\boldsymbol{r} - \boldsymbol{R}_k)(\boldsymbol{r} - \boldsymbol{R}_N)\delta_{uv} - (\boldsymbol{r} - \boldsymbol{R}_N)_u(\boldsymbol{r} - \boldsymbol{R}_k)_v}{|\boldsymbol{r} - \boldsymbol{R}_N|^3}. \tag{7}$$

In the case of the individual gauge for localized orbitals, we obtain

$$\beta_{ak}(v) = \sum_{m}\left\{\frac{\sum_{n}\left(-(1/2c)\langle a|\ell_{nv}|n\rangle + \sum_{j}\langle a|(\Lambda_n - \Lambda_j)_v|j\rangle\langle j|F^0|n\rangle\right)U_{nm}}{e_m - e_a - \Delta E_{m\to a}^{xc}}\right\}U_{km}, \tag{8}$$

where F^0 is the unperturbed DFT hamiltonian operator, U_{km} is a unitary matrix of a transformation from the canonical to localized MOs (indices "m" and "a" correspond to canonical occupied and virtual MOs, respectively and indices "k", "j" and "n" correspond to localized MOs), and

$$(\Lambda_j)_u = -\frac{1}{2c}(\boldsymbol{R}_j \times \boldsymbol{r})_u \tag{9}$$

For $\Delta E_{m\to a}^{xc}$, we write

$$\Delta E_{m\to a}^{xc} = \frac{1}{2}\left(\frac{3}{4\pi}\right)^{1/3}\int \rho^{\uparrow}(r)^{-2/3}\rho_k(r)\rho_a(r)\mathrm{d}r \tag{10}$$

with $\rho_k(r) = \psi_k^*(r)\psi_k(r)$ and $\rho^{\uparrow}(r) = \sum_k^{\mathrm{occ}}\rho_k(r)$.

XPS

For the comparison between calculations for a single molecule of the model and experiments on a solid, we must shift each computed vertical ionization potentials (VIPs), I'_k by a quantity WD as $I_k = I'_k - WD$, to convert to ionization energy I_k relative to the Fermi level, as stated in our previous studies.[4–6]

In order to obtain the accurate CEBEs, we used generalized transition-state (GTS) method. In the GTS method, Willians and *et al.*[14] proposed the extension of Slater's transition-state method[15] and approximated the endothermicity $\Delta E = E(1) - E(0)$ by

$$\Delta E = [F(0) + 3F(2/3)]/4, \tag{11}$$

where $F(\lambda) = \partial E(\lambda)/\partial\lambda$, and λ $(0 < \lambda \leq 1)$ is assumed to be a continuous variable, with $E(0)$ and $E(1)$ denoting the energies of the initial and final states, respectively. For example, for the ionization of an electron from molecular orbital (MO) ϕ_k of interest, λ represents the fraction of electron removed, and according to the Janak theorem,[16] $F(\lambda)$ is the negative orbital energy $\varepsilon_k(\lambda)$. This procedure is applied in the following way. In the unrestricted generalized transition-state (uGTS) method, we removed 2/3 α electron from MO ϕ_k of interest.

For the VIPs of the valence regions, we use the so-called restricted diffuse ionizations (rDI) model which Asbrink *et al.*[17] proposed in the HAM/3 method. In the rDI model, half of the electron is removed evenly from the valence MOs and the negative charge of the resulting orbital energies correspond to calculated VIPs. This allows us to obtain all valence VIPs in a single calculation.

The intensity of valence XPS was estimated from the relative photo-ionization cross section for Al Kα radiation using the Gelius intensity model.[18] For the relative atomic photo-ionization cross section, we used the theoretical values from Yeh.[19]

CALCULATIONS

NMR Chemical Shielding Tensor

In the case of solving the non-linear equations involving a Hartree–Fock-like DFT equation, we think it is the best way to select a better initial condition. We considered molecular models from X-ray diffraction data for α-D-glucose, β-D-glucose, β-D-glucosamine, and cellobiose, respectively. First and second geometry optimizations for saccharide and mono-amino-sugar molecules were performed by semiempirical AM1 method, and at HF/6-31G(d,p) level with the program Gaussian 98,[20] respectively. In the case of the optimizations for the model molecules from the X-ray diffraction data, we fixed the positions of the atoms except for H atoms and optimized the positions of H atoms. For cellulose and chitosan, we also considered the model dimer from X-ray diffraction data, and performed the geometry optimization for the model of the biopolymers by using the AM1 method, and at the HF/6-31G(d,p) level. In the optimization of the molecules, we also fixed the positions of the atoms except for H atoms in glucose unit and all proton positions were optimized. We performed the ^{13}C shielding calculations of the dimer model due to a deMon NMR program. Reference standard tetramethyl silane (TMS) of the ^{13}C shielding was also optimized under the similar calculation level. Figure 1 shows the model molecules of saccharide, monoamino-sugar, cellulose and chitosan, respectively.

Chemical shift calculations were carried out with the program deMon NMR.[7] We used the Perdew–Wang-91 (PW91)[21] exchange correlation potential, the approximation Loc.1 SOS-DFTP, and polarized valence double-ζ (DZVP) basis[22] of (621/41/1*) for C and N, and (41) for H with auxiliary fitting functions labeled (5,2;5,2) for C, N and O, and (5,1;5,1) for H, respectively.

XPS

We used deMon DFT programs[7] to calculate valence XPS and the CEBEs of the cellulose and chitosan using the model dimer molecules obtained in the previous section of NMR calculations. The deMon calculations were also performed with the Perdew–Wang-91 (PW91)[21] exchange correlation potential. In running the deMon program, we used a nonrandom grid and polarized valence double-ζ (DZVP) basis[20] of (621/41/1*) for C and N, and (41) for H with auxiliary fitting functions labeled (5,2;5,2) for C, N and O, and (5,1;5,1) for H.

To simulate the valence XPS of the biopolymers theoretically, we constructed from a superposition of peaks centered on the VIPs. As was done in previous works,[4–7] each peak was represented by Gaussian lineshape functions of an approximated linewidth (0.10 I_k): $I_k = I_k' - WD$.

RESULTS AND DISCUSSION

As shown in the monomer models (α-D-glucose, β-D-glucosamine) for cellulose and chitosan, respectively in Figure 1, the structure of both biopolymers is very similar except the substitution of one OH group in cellulose by NH_2 group in chitosan. In both compounds one can select six non-equivalent carbon (C1–C6) and four non-equivalent oxygen atoms from different functional groups: –O– (O5) which belongs to glucose ring, –O– (O1, O4) which links the adjacent glucose rings, OH (O3) and CH_2OH (O6). According to the experimental results, ^{13}C NMR signals[11,12] show six non-equivalent carbons of C1–C6 for both cellulose and chitosan polymers in Figure 2. For the XPS of the cellulose,[23] experimental CEBEs of O 1s consist of two different –O– and –OH peaks centered at 532.9 and 533.5 eV, respectively, and the C 1s is also due to two kinds of –O–<u>C</u>H–O– and –<u>C</u>H(OH) peaks at 288.1 and 286.7 eV. Therefore we will perform the analysis of the spectra for the biopolymers by deMon DFT[7] calculations using the model dimers.

^{13}C NMR Chemical Shielding Tensor

Saccharides and Amino-Sugar. In Table I, we showed the calculated carbon shielding constants (σ^{d}, σ^{p0}, σ^{p1}, σ^{total}), and chemical shift (δ_{calc}) for α-

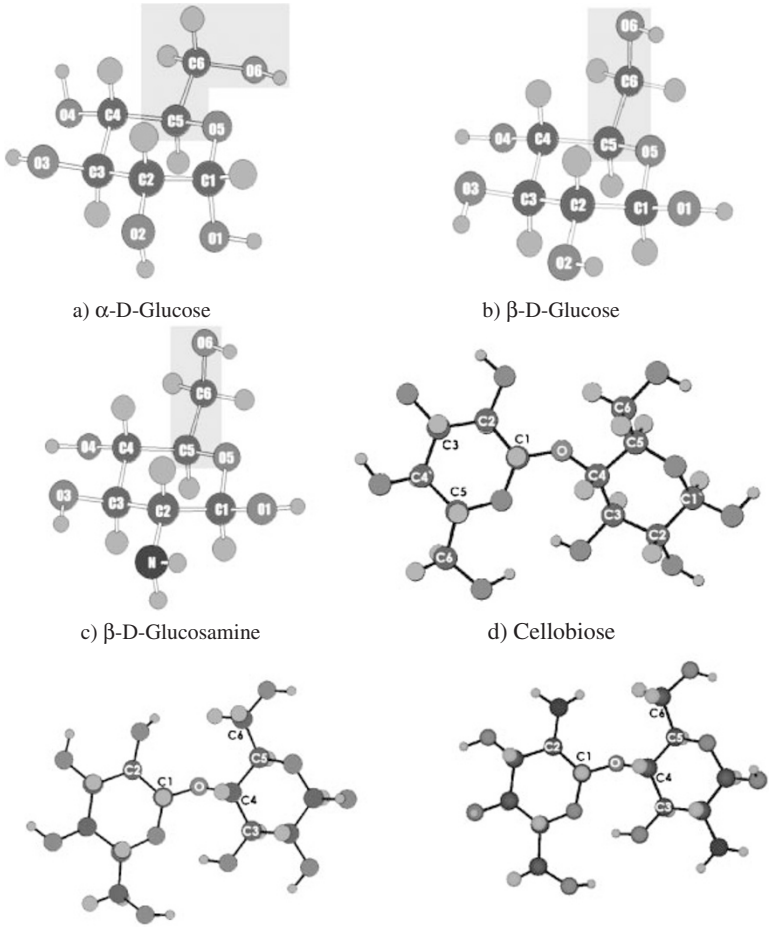

Figure 1. Model molecules of saccharide, mono-amino-sugar, cellulose and chitosan.

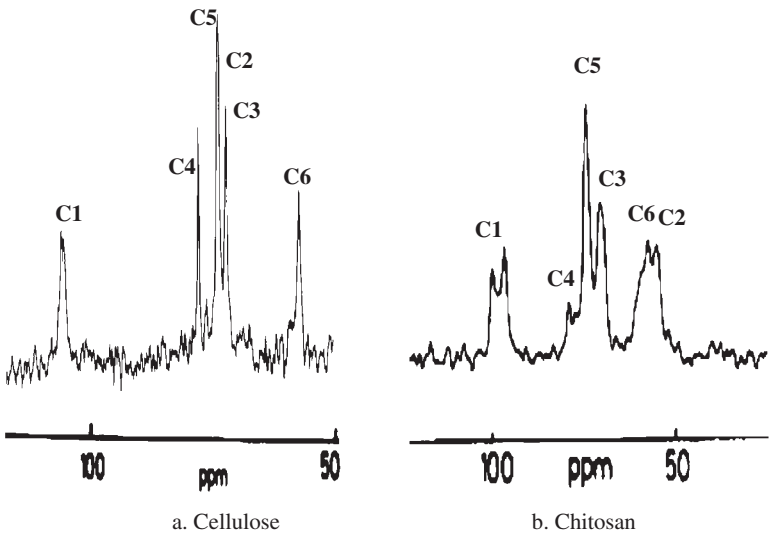

Figure 2. Solid state ^{13}C NMR spectra of cellulose and chitosan.

D-glucose, β-D-glucose and β-D-glucosamine, respectively with the experimental chemical shift (δ_{exp}) referred to the shielding constant of TMS. These compounds were selected to reflect the monomer units in cellulose and chitosan. It can be seen in the table that the calculated chemical shifts (δ_{calc}) of C1–C6 carbons for α-D-glucose, β-D-glucose and β-D-glucosamine are in considerably good accordance in the experimental ^{13}C values (δ_{exp}) in solution in the average absolute deviation (AAD) of ± 3.1 ppm. We can see

Table I. ^{13}C chemical shielding constants of α-glucose, β-glucose and β-glucosamine with the experimental shifts in solution referred to the shielding constant of TMS

α-Glucose						
	C1	C2	C3	C4	C5	C6
σ^{d}	252.0	254.2	254.5	254.5	254.5	253.0
σ^{p0}	35.7	49.6	50.8	50.0	52.0	50.9
σ^{p1}	−143.2	−138.1	−139.4	−139.4	−140.0	−127.6
σ^{total}	144.4	165.7	165.9	165.2	166.5	176.2
δ_{calc}	97.6	76.3	76.2	76.9	75.5	65.8
δ_{exp}	93.4	72.9	73.3	70.8	71.8	63.8
Deviation	+4.2	+3.4	+2.9	+6.1	+3.7	+2.0
β-Glucose						
	C1	C2	C3	C4	C5	C6
σ^{d}	252.0	254.7	254.5	254.4	254.0	253.0
σ^{p0}	34.3	51.0	49.3	51.3	49.1	52.2
σ^{p1}	−144.5	−142.1	−141.6	−132.9	−142.2	−126.1
σ^{total}	141.7	163.6	162.1	172.9	160.9	179.1
δ_{calc}	100.3	78.4	79.9	69.1	81.1	62.9
δ_{exp}	97.6	75.4	76.5	70.3	76.2	61.9
Deviation	+2.7	+3.0	+3.4	−1.2	+4.9	+1.2
β-Glucosamine						
	C1	C2	C3	C4	C5	C6
σ^{d}	251.9	255.9	254.5	254.5	254.1	253.0
σ^{p0}	33.5	57.9	49.4	51.3	49.3	52.2
σ^{p1}	−145.3	−133.1	−140.8	−134.1	−142.1	−126.1
σ^{total}	140.1	180.7	163.1	171.7	161.3	179.1
δ_{calc}	101.9	61.3	78.9	70.3	80.8	62.9
δ_{exp}	95.3	59.5	74.5	72.2	78.6	63.1
Deviation	+6.6	+2.0	+4.4	−1.9	+2.2	−0.2

Table II. ^{13}C chemical shielding constants of cellobiose with the experimental shifts in solid referred to the shielding constant of TMS

Cellobiose						
	C1	C2	C3	C4	C5	C6
σ^{d}	252.2	254.5	254.4	254.0	254.1	253.0
σ^{p0}	34.3	50.8	49.3	49.2	49.4	51.4
σ^{p1}	−152.0	−141.4	−141.9	−151.0	−144.2	−129.0
σ^{total}	127.0	163.8	161.9	152.3	159.4	175.5
δ_{calc}	104.5	75.2	77.2	86.8	79.7	63.6
δ_{exp}	104.6	76.5	78.7	85.5	79.7	63.8
Deviation	−0.1	−1.3	−1.5	+1.3	+0.0	−0.3
	C1′	C2′	C3′	C4′	C5′	C6′
σ^{d}	251.6	254.0	253.9	254.2	254.3	254.5
σ^{p0}	34.0	50.3	49.8	49.9	49.9	50.4
σ^{p1}	−146.8	−139.2	−140.3	−135.5	−139.3	−132.3
σ^{total}	138.8	165.2	163.4	168.6	164.9	172.5
δ_{calc}	100.3	73.9	75.6	70.4	74.1	66.5
δ_{exp}	97.5	76.5	78.7	72.4	79.7	63.8
Deviation	+2.8	−2.6	−3.1	−2.0	−5.6	+2.7

from the calculation result that the chemical shielding of C1–C6 carbons depends on the total paramagnetic shielding constants (σ^{p0} and σ^{p1}), since the diamagnetic term ($\sigma^{d} = 252.0$–254 ppm) of six carbons is almost constant. The shielding orders of carbon nuclei for saccharides and amino-sugar in Table I follow C1 (–O–C̲H(OH)–) > C2–C5 (–C̲H(OH)– or –O–C̲H–C) > C6 (–C̲H$_2$(OH)), and C1 (–O–C̲H(OH)–) > C5 (–O–C̲H–C) > C3, C4 (–C̲H(OH)–) > C6 (–C̲H$_2$(OH)) > C2 (–C̲H(NH$_2$)), respectively.

In order to compare the calculated carbon chemical shifts of the typical disaccharide molecule for cellulose with the experimental values in solid, we used the cellobiose compound shown in Figure 1d. Table II also shows the calculated twelve carbon shielding constants and chemical shifts with the experimental ^{13}C chemical shift values referred to the shielding constant of TMS. The twelve carbon chemical shifts are classified into five species due to the differences among the neighbor oxygen functional groups: C1 carbon which bonded to two ether (–O–) groups is at the lowest-field ($\delta_{exp} = 104.6$ ppm), C1′ carbon which has –O– and –OH groups exists at the next lower field ($\delta_{exp} = 97.5$ ppm), C4 which bonded to one –O– group is observed at the second next low field ($\delta_{exp} = 85.5$), carbons in –CH(OH) group are in the range of $\delta_{exp} = 72.4$–79.7 ppm, and carbons in –C̲H$_2$(OH) group is at the highest field ($\delta_{exp} = 63.8$ ppm). The calculated results correspond well to the order of the experimental ones in solid in AAD of ±1.9 ppm. For the result of cellobiose, the chemical shielding of twelve carbons is also seen to be determined dominantly with the total paramagnetic shielding constants.

Cellulose and Chitosan. In Table III, we showed the calculated twelve carbon shielding constants and chemical shifts of the dimer models for cellulose and chitosan with the six experimental ^{13}C shift values referred to the shielding constant of TMS. In the table, we adopted experimental ^{13}C values of C4′ and C4 for cellobiose and β-D-glucosamine, respectively in comparison of the calculated C4′ values of the model molecules with it, because the C4′ carbon of the model molecules bonds to the –OH group. Then, the calculated values exist in the ADD range of ±3.1 ppm for both cellulose and chitosan, and are also in good accordance with experimental ones. The carbon NMR chemical shielding is also dominated by the total paramagnetic shielding constants, since the diamagnetic shielding constants are almost similar values.

In the table, the shifts of C1 and C1′ carbons bonded to two oxygen atoms are much lower field than all other carbons in cellulose and chitosan. For C4 and C6 carbons of both models, the former carbon shift bonded to an ether group is at the lower field, while the latter carbon in –C̲H$_2$(OH) group exists in the higher

Table III. ^{13}C chemical shielding constants of model dimmers for cellulose and chitosan with the experimental shifts referred to the constant of TMS

	Cellulose					
	C1	C2	C3	C4	C5	C6
σ^{d}	252.0	254.2	254.4	254.2	254.3	253.4
σ^{p0}	34.2	50.6	50.0	48.5	49.7	53.2
σ^{p1}	−159.2	−143.3	−143.2	−153.0	−146.3	−128.9
σ^{total}	127.0	161.5	161.2	149.7	157.8	177.7
δ_{calc}	112.1	77.6	77.9	89.3	81.2	61.4
δ_{exp}	107.1	73.4	76.0	88.9	77.7	64.0
Deviation	+5.0	+4.2	+1.9	+0.6	+3.5	−2.6
	C1′	C2′	C3′	C4′	C5′	C6′
σ^{d}	251.4	254.1	254.4	253.7	254.3	253.5
σ^{p0}	33.9	49.6	50.0	49.5	49.8	52.6
σ^{p1}	−147.6	−144.4	−143.2	−135.8	−146.0	−129.1
σ^{total}	137.7	159.3	161.1	167.4	158.1	176.9
δ_{calc}	101.4	79.7	77.9	71.7	80.9	62.1
δ_{exp}	107.1	73.4	76.0	(72.4)[a]	77.7	64.0
Deviation	−5.7	+6.3	+1.9	(−0.7)	+3.2	−1.9
	Chitosan					
	C1	C2	C3	C4	C5	C6
σ^{d}	251.0	254.5	253.2	253.6	253.4	251.7
σ^{p0}	31.9	56.7	47.4	47.7	49.4	50.0
σ^{p1}	−159.5	−131.1	−143.7	−153.6	−143.8	−130.9
σ^{total}	123.4	180.2	157.1	147.7	159.0	170.8
δ_{calc}	115.6	58.8	81.9	91.3	80.0	68.2
δ_{exp}	110.0	62.4	80.8	86.6	80.8	65.6
Deviation	+5.6	−3.6	+1.1	+4.7	−0.8	+2.6
	C1′	C2′	C3′	C4′	C5′	C6′
σ^{d}	250.7	254.6	253.5	253.4	253.1	251.7
σ^{p0}	32.7	56.2	48.6	48.7	49.2	49.6
σ^{p1}	−149.4	−135.0	−141.1	−140.9	−141.7	−130.8
σ^{total}	133.9	175.9	160.9	161.2	160.6	170.5
δ_{calc}	105.1	63.1	78.1	77.8	78.4	68.5
δ_{exp}	110.0	62.4	80.8	(72.2)[b]	80.8	65.6
Deviation	−4.9	+0.7	−2.7	(+5.6)	−2.4	+2.9

[a]The value was referred from experimental ^{13}C shift of C4′ of cellobiose in Table II. [b]The value was referred from experimental ^{13}C shift of C4′ of β-glucosamine in Table I.

field. These results correspond to tendency of C1, C1′, C4 and C6 for cellobiose. In the case of C2 and C2′ carbons for both polymers, the carbon nuclei in –CH(NH_2) group of chitosan are at the highest field of all carbons. The reason is due that the total paramagnetic terms of C2, C2′ carbons in chitosan model have much higher values than those terms in cellulose model, since the diamagnetic term is almost constant value (σ^{d} = 251–255 ppm).

XPS

Valence XPS. It is interesting to discuss the experimental spectrum in detail from a theoretical viewpoint. We showed the theoretical valence spectra of cellulose and chitosan by deMon DFT calculations using the dimer models with experimental ones in Figures 3a and b, respectively. The simulated results for cellulose and chitosan are in considerably good accordance with the experimental ones in the figure. Tables IV and V summarized the experimental peaks, calculated VIPs, main atomic orbital (AO) photoionization cross-sections (PICS), orbital nature and functional group. In Figures 3a and b, the intense peaks at around 26 eV are due mainly to sσ (O 2s–C 2s) bonding of –O–C group for the biopolymers. We can find out from simulation spectra of the figure that the difference of the spectra between cellulose and chitosan is in the energy range of 21–23 eV. In the case of chitosan, the shoulder peak at around 22 eV results from the sσ (N 2s–C 2s) bonding of H_2N–C group. Broader and shoulder peaks in the range of 13–20 and 3–13 eV result dominantly from

a) Cellulose

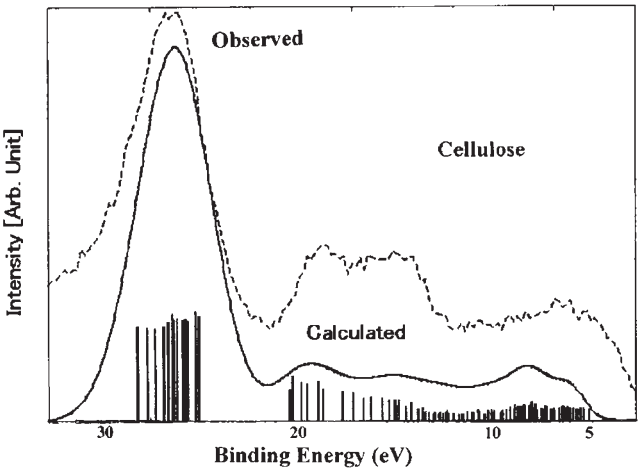

b) Chitosan

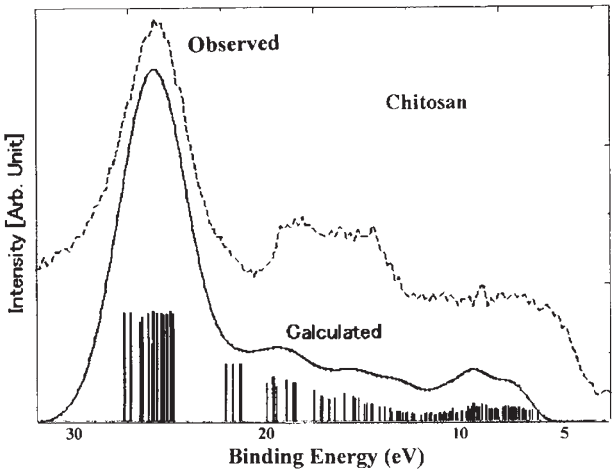

Figure 3. Valence XPS of cellulose and chitosan.

Table IV. Observed peaks, VIP, main AO PICS, orbitals nature and functional group for valence XPS of cellulose (Shift between the observed and calculated VIP is 5.0 eV)

Peak (eV)	VIP (eV)	Main AO PICS	Orbital nature[b]	Functional group
26 (30–23)[a]	30.8–28.4	O 2s	sσ(O 2s–C 2s)–B	–O–C
19 (21–18)[a]	23.5–22.5	C 2s O 2s	sσ(C 2s–C 2s)–B	–C–C
15 (18–13)[a]	21.0–13.0	O 2s O 2p	pσ(O 2s–C 2p)–B pσ(C 2s–O 2p)–B	–C–O –O–C
8 (13–3)[a]	14.0–13.0 12.5–11.7 10.5–9.1	C 2p O 2p C 2p O 2p O 2p	pσ(O 2p–C 2p)–B pσ(O,C 2p–O,C 2p)–B pπ(Lone Pair)–NB	–O–C –C–O, –C–C –O–

[a]Peak range

Table V. Observed peaks, VIP, main AO PICS, orbitals nature and functional group for valence XPS of chitosan (Shift between the observed and calculated VIP is 5.0 eV)

Peak (eV)	VIP (eV)	Main AO PICS	Orbital nature[b]	Functional group
26 (30–21)[a]	30.4–28.1 25.0–24.6	O 2s N 2s	sσ(O 2s–C 2s)–B sσ(C 2s–N 2s)–B	–O–C –N–C
19 (20–17)[a]	22.9–21.8	C 2s	sσ(C 2s–C 2s)–B pσ(C 2s–O 2p)–B	–C–C –C–O
16 (17–13)[a]	20.5–17.6	O 2p C 2p	pσ(C 2s–O 2p)–B	–C–O
8 (13–3)[a]	12.5–11.5 10.3–8.8 8.5–8.1	C 2p O 2p O 2p N 2p	pσ(O,C 2p–O,C 2p)–B pπ(Lone Pair)–NB pπ(Lone Pair)–NB	–C–O, –C–C– –O– –N–

[a]Peak range

pσ bonding and pπ (lone-pair) non-bonding, respectively for both polymers.

Furthermore, we examined contribution of each atom for the simulated spectra in Figures 4a and b. It can be seen in the figure that the intense peak at around 26 eV is due to the oxygen, and (oxygen and nitrogen) atoms for cellulose and chitosan, respectively. For both polymers, the carbon contribution is a little larger than oxygen one for broader peak in the range of 13–20 eV. In the case of broader peak between 3.0 (or 5.0) and 13 eV, the oxygen contribution also seems to dominate.

CEBEs of the Biopolymers

Table VI shows the CEBEs of the model monomers for the biopolymers using the uGTS method with scaled-pVDZ basis. In the table, we showed the *WD* values of the polymers from the differences between calculated CEBE values for the model molecules and experimental ones on the solid polymers. We, thus, estimated as 5.9 and 5.7 eV for averaged ***WD*** values of cellulose and chitosan, respectively. The *WD*s from the CEBEs are the most reliable, as described in previous works.[4]

CONCLUSIONS

We have analyzed ^{13}C NMR chemical shielding and valence XPS of cellulose and chitosan by deMon DFT calculations using the model dimers.

For ^{13}C NMR chemical shielding, the calculated chemical shifts of (α-D-glucose, β-D-glucose, and β-D-glucosamine) and cellobiose with DZVP basis are in considerably good accordance with the experimental values in the average absolute deviations (AAD) of ±3.1 and 2.0 ppm, respectively. The calculated ^{13}C shifts of the dimer models correspond well to the experimental ones of both solid polymers in the AAD of ±3.1 ppm. The carbon NMR chemical shielding is also dominated by the total paramagnetic shielding constants, since the diamagnetic shielding constants are almost similar values.

The simulated valence spectra of the dimer models using the restricted diffuse ionization (rDI) method showed good agreement with the experimental ones of cellulose and chitosan. We obtained the reasonable

a) Cellulose

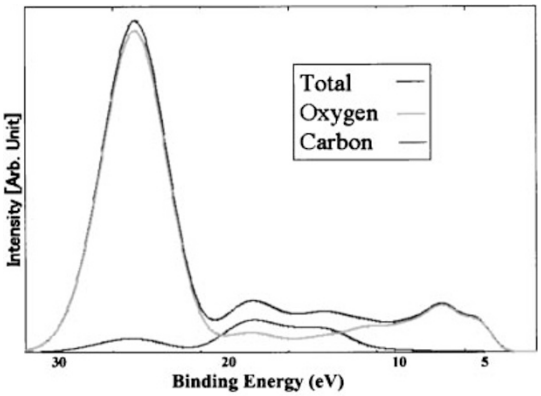

b) Chitosan

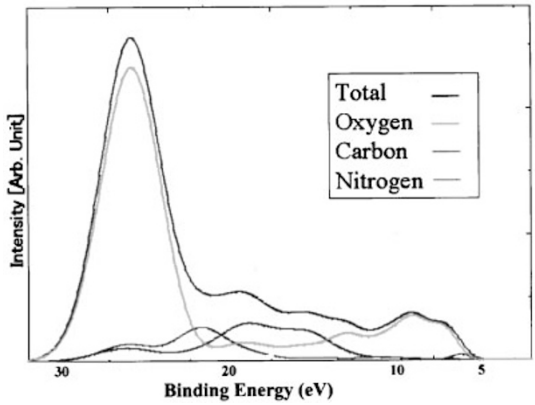

Figure 4. Each atom contribution for valence XPS of cellulose and chitosan.

Table VI. CEBEs (in eV) of biopolymers by deMon calculations using model dimers

Polymers	Obsd.	Model molecule	
		Calc.	*WD*
Cellulose			
C 1s [O–CH–O]	288.1	294.3	6.2
C 1s [–CH(OH)–]	286.7	292.5	5.8
O 1s [–O–]	533.5	539.3	5.8
O 1s [–OH]	532.9	538.5	5.6
Chitosan			
C 1s [O–CH–O]	288.0	294.2	6.2
C 1s [–CH(OH)–]	286.6	292.5	5.9
O 1s [–O–]	533.5	538.8	5.3
O 1s [–OH]	533.0	538.6	5.6
N 1s [–NH_2–]	399.3	404.6	5.3

WD values of cellulose and chitosan as 5.9 and 5.7 eV, respectively from the differences between calculated CEBE values for the monomer model molecules and experimental ones on the solid polymers.

REFERENCES

1. R. A. A. Muzzarelli, "Natural Chelating Polymers," Pergamon, Oxford, U.K., 1973.
2. K. Endo, I. Fujita, and N. Kobayashi, *Anal. Sci.*, **7**, 785 (1991).
3. T. Hoshiba, T. Ida, M. Mizuno, T. Otsuka, K. Takaoka, and K. Endo, *J. Mol. Struct.*, **602–603**, 381 (2002).
4. K. Endo, Y. Kaneda, H. Okada, D. P. Chong, and P. Duffy, *J. Phys. Chem.*, **100**, 19455 (1996).
5. S. Shimada, T. Ida, K. Endo, S. Suhara, E. Z. Kurmaev, and D. P. Chong, *Polym. J.*, **32**, 1030 (2000).
6. K. Endo, S. Shimada, T. Ida, S. Suhara, E. Z. Kurmaev, A. Moewes, and D. P. Chong, *J. Mol. Struct.*, **561**, 17 (2001).
7. a) A. St-Amant and D. R. Salahub, *Chem. Phys. Lett.*, **169**, 387 (1990).
   b) A. St-Amant, Ph. D. Thesis, University of Montreal, 1991.
8. E. Piron and A. Domard, *Int. J. Biol. Macromol.*, **22**, 33 (1998).
9. F. Horii, A. Hirai, and R. Kitamaru, *Polym. Bull.*, **10**, 357 (1983).
10. E. Guibal, C. Milot, O. Eterradossi, C. Gauffier, and A. Domard, *Int. J. Biol. Macromol.*, **24**, 49 (1999).
11. R. L. Dudley, C. A. Fyfe, P. J. Stepheson, Y. Deslamdes, G. K. Hamer, and R. H. Marchessault, *J. Am. Chem. Soc.*, **105**, 2469 (1983).
12. H. Saito, R. Tabeta, and K. Ogawa, *Macromolecules*, **20**, 2424 (1987).
13. V. G. Malkin, O. L. Malkina, M. E. Casida, and D. R. Salahub, *J. Am. Chem. Soc.*, **116**, 5898 (1994).
14. A. R. Williams, R. A. deGroot, and C. B. Sommers, *J. Chem. Phys.*, **63**, 628 (1975).
15. J. C. Slater, *Adv. Quantum Chem.*, **6**, 1 (1972).
16. J. F. Janak, *Phys. Rev. A*, **18**, 7165 (1978).
17. E. Lindholm and L. Asbrink, "Molecular Orbitals and their Energies Studied by the Semiemprical HAM Method," Springer-Verlag, Berlin, 1985.
18. a) U. Gelius and K. Siegbahan, *Faraday Discuss. Chem. Soc.*, **54**, 257 (1972).
    b) U. Gelius, *J. Electron Spectrosc. Relat. Phenom.*, **5**, 985 (1974).
19. J. J. Yeh, "Atomic Calculation of Photoionization Cross Section and Asymmetry Parameters," Gordon & Breach Science Publishers, Langhorne, PA, 1993.
20. M. J. Frisch, G. W. Trucks, H. B. Schlegel, G. E. Scuseria, M. A. Robb, J. R. Cheeseman, M. C. Strai, J. C. Burant, R. E. Stratmann, S. Dapprich, K. N. Kudin, J. M. Millam, A. D. Daniels, G. A. Petersson, J. A. Montgomery, V. G. Zakrzewski, K. Raghavachari, P. Y. Ayala, Q. Cui, K. Morokuma, J. B. Foresman, J. Cioslowski, J. V. Ortiz, V. Barone, B. B. Stefanov, G. Liu, A. Liashenko, P. Piskorz, W. Chen, M. W. Wong, J. L. Andres, E. S. Replogle, R. Gomperts, R. L. Martin, D. J. Fox, T. Keith, M. A. AlLaham, A. Nanayakkara, M. Challacombe, C. Y. Peng, J. P. Stewart, C. Gonzalez, M. Head-Gordon, P. M. W. Gill, B. G. Johnson, and J. A. Pople, Gaussian-98, Revision

Gaussian, Inc., Pittsburgh, PA, 1998.

21. a) J. P. Perdew and Y. Wang, *Phys. Rev. B*, **45**, 13244 (1992).
    b) J. P. Perdew, in "Electronic Structure of Solids," P. Ziesche and H. Eischrig, Ed., Akademie-Verlag, Berlin, 1991.
    c) J. P. Perdew, J. A. Chevary, S. H. Vosko, M. R. Pederson, D. J. Singh, and C. Foilhais, *Phys. Rev. B*, **46**, 6671 (1992).
22. T. H. Dunning Jr. and P. J. Hay, "Methods of Electronic Structure Theory," Plenum Publishing, New York, N.Y., 1977.
23. G. Beamson and D. Briggs, "High Resolution XPS of Organic Polymers. The Scienta ESCA 3000 Database," John Wiley & Sons, Inc., Chichester, U.K., 1992.